Journal of Minerals and Materials Characterization and Engineering, 2016, 4, 62-72
Published Online January 2016 in SciRes. http://www.scirp.org/journal/jmmce
http://dx.doi.org/10.4236/jmmce.2016.41007

Characterization of Surface State of Inert Particles: Case of Si and SiC

Désiré M. K. Abro[1], Pierre Dablé[2], Fernando Cortez-Salazar[3], Véronique Amstutz[3], Hubert Girault[3]

[1]Laboratoire de Chimie Physique, Université F. H. B. Cocody, Abidjan, Côte d'Ivoire
[2]Laboratoire de Thermodynamique de Traitement et Sciences des Surfaces et Interfaces, Institut National Polytechnique F.H.B., Yamoussoukro, Côte d'Ivoire
[3]Laboratoire d'Electrochimie Physique et Analytique, Ecole Polytechnique Fédérale de Lausanne, Sion, Suisse
Email: abrodesire@hotmail.com

Received 26 December 2015; accepted 25 January 2016; published 28 January 2016

Abstract

Silicon and Silicon carbide particles have been investigated by the mean of infrared (IR) spectroscopy and X-ray photoelectron spectroscopy (XPS) to establish their surface states. The results of this research are based on the estimation of the area under the high resolution peaks by isosceles triangles. This approach leads to the repartition of the particles surfaces in term of atomic percentage and of type of bonds. The surface of silicon particles is divided up into 54.85% of Si-O bonds and 36.85% of Si-Si bonds. The remaining surface is constituted of zeolite, the raw material used to produce the silicon particles. The surface of silicon carbide particles consists of 50.44% of Si-C bonds, 24.01% of Si-O bonds and 25.55% of graphite. 10.01% of the graphite is derived from the oxidation of Si-C bonds while 11.48% is due to contamination. The zeta potential evolution versus pH confirms the distribution of chemical groups found.

Keywords

IR and XPS Sprectra, Si, SiC, Surface State, Zeta Potential

1. Introduction

Silicon (Si) and silicon carbide (SiC) particles are widely used in energy storage, electronic applications and to improve anticorrosion or mechanical properties of materials. In various processes such as the preparation of ceramics and electrolytic codeposition [1] [2], they are generally suspended in solution with surfactants before their use in the process. This crucial step may prove disastrous if suspensions form precipitates.

How to cite this paper: Abro, D.M.K., Dablé, P., Cortez-Salazar, F., Amstutz, V. and Girault, H. (2016) Characterization of Surface State of Inert Particles: Case of Si and SiC. *Journal of Minerals and Materials Characterization and Engineering*, **4**, 62-72. http://dx.doi.org/10.4236/jmmce.2016.41007

Such behavior of the particles will necessarily lead to the production of materials of lower mechanical quality [3]-[6]. Thus, determination of their chemical evolution and the definition of conditions that can ensure the stability of these phases are required. This investigation is essentially based on the characterization of the nature of surface functional groups of these inert particles.

Particle surfaces are likely to be constituted of functional groups, as a result either the preparation process or their interactions with their environment. In solutions, these groups may influence significantly the chemical and physical behaviour of solid particles [7], owing to their specific reactivity with the solvent or other species present in the solution. Therefore, it is fundamental to characterize these functional groups and, when possible, their surface distribution for understanding and interpret these behaviors in a given solution.

In this study, infrared (IR) spectroscopy and X-rays photoelectron spectroscopy (XPS) analysis were performed for a thorough understanding of the surface of silicon (Si) and silicon carbide (SiC) particles. While IR spectroscopy has provided access to the surface functional groups, XPS spectroscopy has allowed determining, for each element present at the surface of the samples, its atomic percentage and the nature of bonds with the surrounding atoms. The change of zeta-potential of particles as a function of pH has also highlighted the nature of their interactions with the species in solution. A compilation of these information has greatly contributed to characterize particle surfaces in terms of their chemical composition and to elucidate their interactions with their environments.

2. Materials and Methods

2.1. Specific Surface

The particles used in these studies are silicon (Si, 99.9%, Alfa Aesar), the size of which ranges from 1 to 5 µm and silicon carbide (SiC, Goodfellow), of a size of 0.1 to 1 µm (**Figure 1**).

The specific surfaces of the particles were determined by the Brunauer-Emmett-Teller (BET) isotherm, which is based on the adsorption and desorption of nitrogen molecules [8]. This experiment was run by the instrument GEMINI 2375 MICROMERITICS.

2.2. Infrared Spectroscopy (IR)

The IR spectra were performed using a Perkin Flower apparatus, controlled by a SPECTRUM software. Infrared radiations are sent to the samples of silicon and silicon carbide particles directly without immerse them first in any solution. The different vibrations are recorded as a function of wavenumbers. IR spectra are analysed even in the fingerprints zone; *i.e.* for wavenumber lower than 1500 cm^{-1}.

2.3. X-Ray Photoelectron Spectroscopy (XPS)

The global and high-resolution XPS spectra were measured with an AXIS ULTRA apparatus. The different kinds of atoms present at the particles surfaces and their surface concentrations in atomic percent and in mass

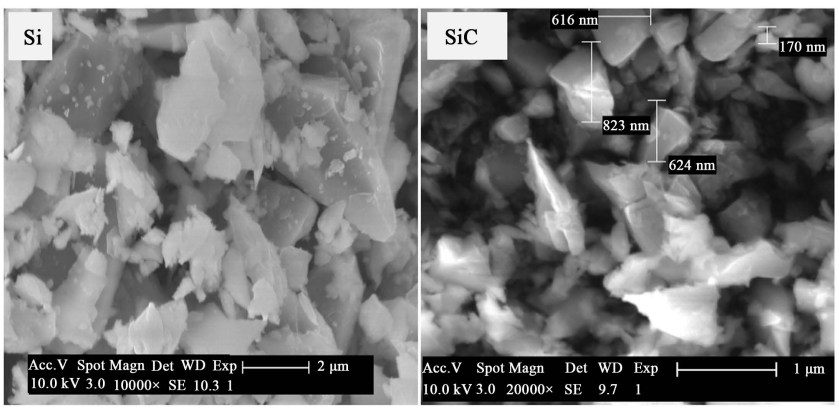

Figure 1. SEM pictures of silicon (Si) and silicon carbide (SiC) particles.

percent were determined from the global spectra. The high-resolution spectra for each particles are also provided. Since the binding energy is characteristic of the number and the different types of bonds related to a specific element, informations about surface states will be extracted using the isosceles method. For each peak of the spectrum, the area defined by the isosceles triangle integrating the top of the peak is proportional to the number of bonds present at the surface of the particles. To this end, the whole set of high-resolution spectra should be presented in the same scale to obtain comparable surfaces. Therefore, the sum of these peak areas corresponding to 100% of the bonds, can be correlated to surface of the particle studied. On the basis of the percentage of each bonds detected by XPS, the area distribution of the different bonds can be calculated.

2.4. Zeta Potential

Zeta-potentials were measured for each type of particle in colloidal solutions containing 0.5 g/L of particles and sodium chloride (99.5%, Fluka) at a concentration of 10^{-2} mol/L, prepared with previously deoxygenated and deionized water. Solutions were prepared for different pH values, comprised between 2.5 and 5. The zeta-potential values were determined using the Zetasizer apparatus Nanoseries ZS from Malvern Instruments.

3. Results and Discussions

3.1. Specific Surfaces

The specific surfaces determined by BET method are presented in **Table 1**. The specific surface area represents the real surface of the particles for a mass of one gram. This non-intrinsic quantity is particularly related to the procedure of preparation of the powder [9].

The analysis of the data provided in **Table 1** shows that, as expected, the specific surface area of the particles is in inverse relationship with their particle size. Thus, the SiC powder exhibits a higher surface area than the Si powder, due to its lower size.

3.2. IR Spectra

3.2.1. IR Spectrum of Silicon

The IR spectra recorded for Si particles is presented in **Figures 2(a)**.

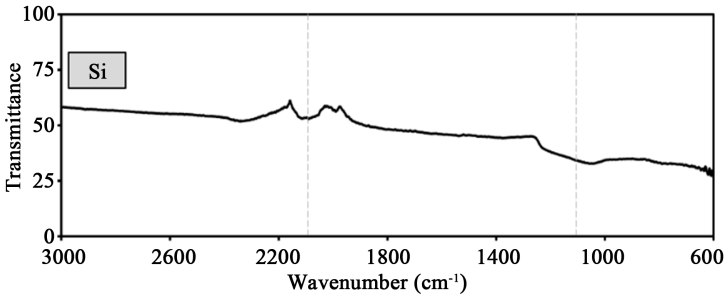

(a)

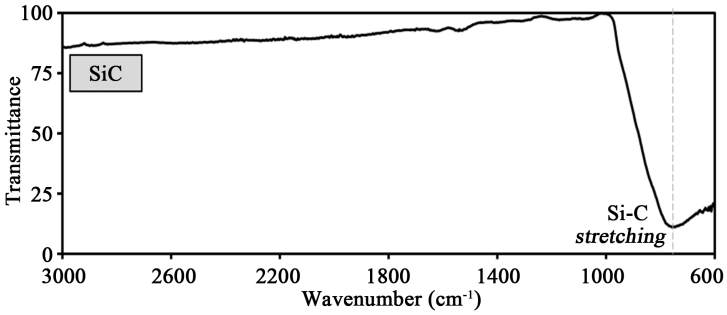

(b)

Figure 2. (a) IR spectrum of Si particles; (b) IR spectrum of SiC particles.

Table 1. Specific surface area of commercially available Si and SiC particles, as determined by the BET isotherm.

Particle	Size (µm)	Specific area ($m^2 \cdot g^{-1}$)
Si	1 - 5	5.7
SiC	0.1 - 1	21.30

In **Figure 2(a)**, no absorption peak is clearly defined although a transmission band characteristic of the Si-O bonds in the wave number range of 800 and 1200 cm^{-1} was is expected [10]. This is related to the homo-atomic structure of this phase. In fact, the sensitivity of infrared spectroscopy is more pronounced for hetero-atomic groups. However, the transmittance lower than 100% on the wavenumber window swept may indicate the presence of oxygen at the surface of the particles due to the interactions between the silicon atoms and the oxygen present in the environment.

A band at higher wave numbers, centred on 2093 cm^{-1} was also observed on the IR spectrum of Si particles. This corresponds to the presence of a Si-H group [11], which could originate from contaminations during the preparation process of these particles.

3.2.2. IR Spectrum of Silicon Carbide

The recorded IR spectrum for the SiC particles is characterized by a unique, wide and intense absorption band, centered around 780 cm^{-1} (**Figure 2(b)**).

This band is characteristic of the Si-C bond. At higher wavenumbers, until 3000 cm^{-1}, the spectrum does not exhibits any significant peak which would indicate any other functional group.

3.3. XPS Spectra

Two types of XPS spectra have been recorded for each material: the general spectrum and the high resolution spectrum. The resonance peaks of the general spectrum can be correlated to the chemical bonds and consequently species present at the surface of the particles. Their relative mass and atomic percentages are also determined. The high resolution spectrum is performed for each chemical element detected in the general spectra. It based on the deconvolution of the resonance peaks of core level electrons *s* and *p* for each elements. The peak energy values of these photoelectrons for a specific element indicate the type of bond and the nature of the atoms to which it is bonded. The characterization of the surface consists of the determination of chemical species present thereon and their corresponding surface proportions. The set of atomic percentages originating from the general spectrum provides, by counting, the number of photoelectrons emitted at a specific excitation applied.

3.3.1. General and Hihg Resolution XPS Spectra of Silicon Particles

The spectrum obtained from the XPS analysis of the silicon particles shows peaks characteristic of silicon, oxygen and carbon atoms (**Figure 3**).

These peaks are followed on their left side by tails of lower intensities. The latters result from lower energy photoelectrons detected. The lose energy are due to inelastic shocks occured before photoelectron detections [12]. The presence of silicon on the surface is materialized by the Si_{2s} and Si_{2p} peaks around 160 eV and 100 eV respectively. The signal for silicon is split in two peaks as two electrons are emitted from its *p* and *s* atomic layers. This duplication is shown more precisely in the inset of **Figure 3**.

Besides the Si signal, an intense peak is observed at 533.06 eV and a smaller one at 555.1 eV. The first one corresponds to the emission of a photoelectron from the O_{1s} layer, confirming the presence of oxygen at the surface of the particles. The peak at 555.1 eV O_{KLL} corresponds to the emission of backscattered Auger electrons by oxygen atoms. The presence of carbon atoms at the surface of Si particles is revealed by a very low intensity C_{1s} peak at 285 eV. This carbon could arise from a contamination due to adsorption of (hydro)carbon compounds or an impurity in the material. These results are in agreement with those obtained by Moreau [13] and J. Binner [14].

The presence of adsorbed species that are oxygen and carbon confirm the lower transmittance obtained from silicon particles IR spectrum.

The atomic and mass composition extracted from the general spectrum are shown in **Table 2**.

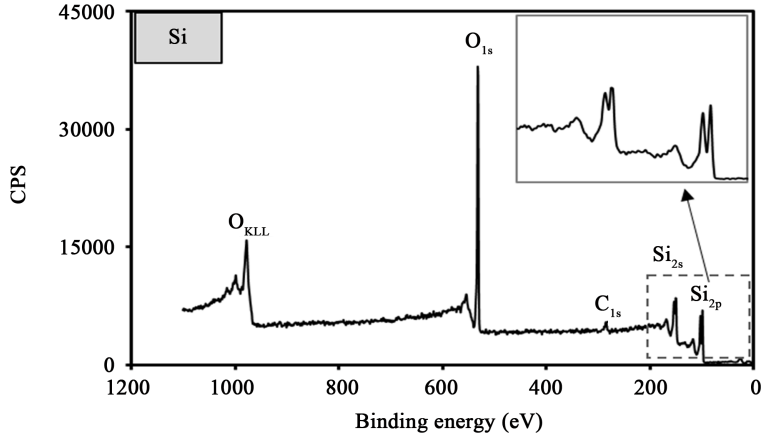

Figure 3. XPS general spectrum of silicon particles.

Table 2. Silicon particles surface composition.

	O	C	Si
Atomic %	45.25	7.75	47.00
Mass %	33.88	4.35	61.76

The high resolution spectra extracted from the general spectrum are shown in **Figure 4**.

The silicon Si_{2p} HR spectrum indicates the existence of Si-Si bonds at around 99 eV [14]. This peak characterizes the cristalline silicon phase. The presence of Si-O bond is confirmed by the peak at 103 eV on the Si_{2p} spectrum and the peak at 533 eV on the oxygen O_{1s} spectrum. The silicon Si_{2p} spectrum also shows a peak at 107 eV corresponding to a typical Si-O bond of an aluminosilicate phase, in this particular case, the zeolite [15].

The relatively low intensity of this peak may reflect an amorphous structure of this phase. This zeolite phase could originate from the silicon preparation procedure. The zeolite might have served as raw material.

The presence of carbon at the surface of the Si particles is demonstrated by the carbon C_{1s} spectrum with a C-C peak positioned around 285 eV. The presence of C-O bonds is also suggested by the low energy peak at around 286.5 eV on the same spectrum.

The HR spectrum O_{1s} of oxygen confirms the Si-O noticed in Si_{2p} spectrum. The Si-O bonds arise from the interaction of some silicon atoms on the surface with oxygen from the atmosphere.

This spectrum also shows a peak at 536.5 eV, typical of C-O bonds. These last bonds may result from a fraction of the graphite that reacts with oxygen to establish equilibrium with atmosphere since this reaction is thermodynamically favored. Thus, the surface of the silicon particles is constituted of oxygen that thereby reduce the oxygen gradient against this phase.

The overall results of the XPS experiments conduct to the conclusion that the surface of the silicon particles is composed of atoms of silicon, oxygen and carbon. However, the low intensity of the C_{1s} energies indicated on HR spectrum shows that carbon atoms are not strongly bound to the Si surface, on the contrary with silicon and oxygen atoms.This carbon can therefore be considered as a contaminant.

The total surface of the particles can be determined by summing the area of the bonds of the Si_{2p} spectum, with the O-C area on the O_{1s} spectrum and with the C-C area from de C_{1s} spectrum. **Table 3** summarizes the values of the surfaces and the proportions of different types of bonds.

According to **Table 3**, silicon particles are highly oxydized. Si-O bonds cover about 54.85% of their surfaces. Aside the fact that silicon oxidation is thermodynamically favoured according to its negative Gibbs energy *i.e.* $-857\ KJ{\cdot}mol^{-1}$, the oxydation of silicon particles is due to the cristallographic configuration of atoms. Then, on pure silicon surfaces, the atoms located in the outermost atomic layer are not in the tetrahedral configuration (**Figure 5(a)**). Instead, they are engaged in a square-based pyramid (**Figure 5(b)**) in which the binding energies are higher than in the tetrahedron lattice. This is related to the angle of the polyhedron, which is smaller than

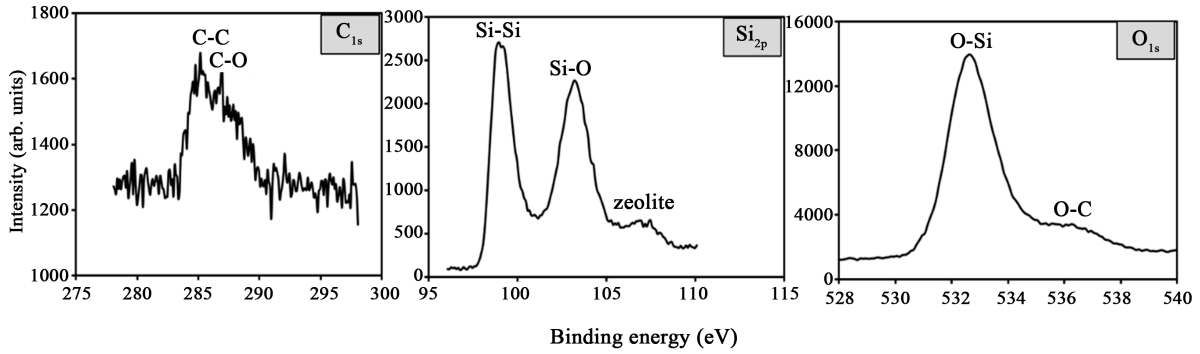

Figure 4. High resolution spectra of silicon particles.

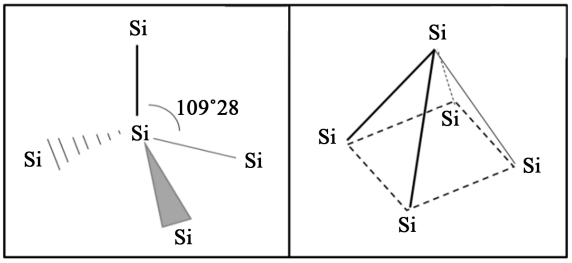

(a) (b)

Figure 5. Tetrahedral (a) and pyramidal (b) configurations of Si at the surface.

Table 3. Distribution in percentage of surface bonds and atomic fraction at Si surface.

	Area (%)	Atomic Fraction (%)
Si-Si	36.85	20.87
Si-O	54.85	23.56
Al_nSiO_m; (zeolite)	4.52	2.56
Total Si (%)		**47**
C-C	3.03	1.38
C-O	14	6.37
Total C (%)		**7.75**
TOTAL (%)	**100**	

109.28˚, rendering the structure less stable. Thus, part of these atoms react with oxygen to decrease the energetic level of the surface Si bonds in order to partly relax the surface atomic layer.

3.3.2. General and High Resolution XPS Spectra for Silicon Carbide Particles

The spectra obtained from the XPS analysis of the SiC particles (**Figure 6**), presents the typical intense peaks of Si_{2s}, Si_{2p}, O_{1s}, O_{KLL} and C_{1s}, corresponding to the atoms of silicon, oxygen and carbon present at their surface.

The surface of these particles is also characterized by the presence of oxygen atoms, which reflect the apparition of a binding oxygen species responsible for the equilibrium of the SiC surface with the atmospheric oxygen.

The peaks of silicon and carbon have almost the same height with respect to the backgound; around 9000 CPS, indicating that the species are in the stoichiometric proportions in the compound.

Table 4 provides atomic and mass proportions of the surface for carbon, silicon and oxygen.

The carbon C_{1s} spectrum exhibits two types of bonds: the C-Si bonds at 282.8 eV [16] characteristic of the silicon carbide phase and the C-C bonds at 285 eV (**Figure 7**).

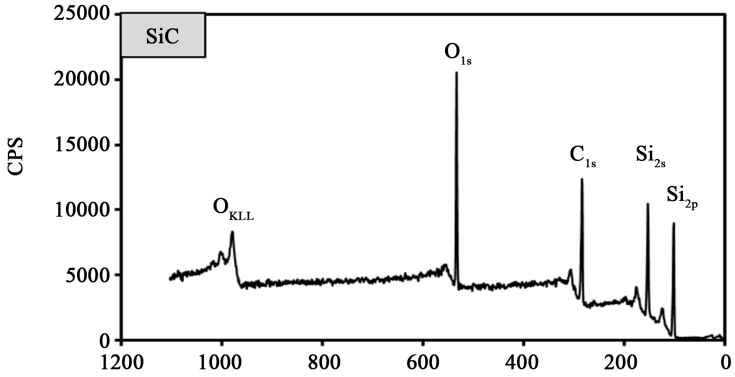

Figure 6. XPS general spectrum of silicon carbide particles.

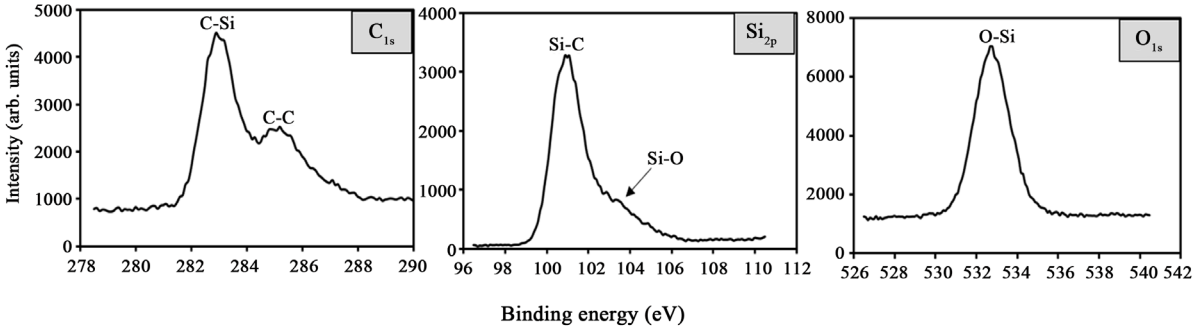

Figure 7. High resolution spectrum of SiC particles.

Table 4. Silicon carbide surface composition.

	O	C	Si
Atomic%	20.02	45.73	34.25
Mass%	17.49	29.99	52.52

However, the intensity of the C-C line is higher than that obtained in the case of the silicon particles. Carbon atoms originate from an another source. G. Ramis *et al.* [17] have shown that the C-C bonds on the SiC particle surfaces are produced by the oxidation of Si-C bonds. A substitution reaction can occur as follows (Equation (1)):

$$\mathrm{Si-C}+\frac{1}{2}\mathrm{O_2}\rightarrow \mathrm{Si-O+C} \quad (1)$$

Thus, the carbon phase characterized by C-C bonds is derived.

Hence, the reaction of Equation (1) leads to O-Si-O groups and results in the silica formation.

By taking into account the stoichiometry of O-Si-O bonds and the amount of surface oxygen namely 20.02 at%, one can estimate at 10.01 at% the silicon atoms involved in this phase. In accordance with the oxidation reaction of the SiC (Equation (1)), the amount of silicon oxidized equals that of the released carbon. In fact, from the total carbon percentage, that is 45.73 at% (**Table 4**), 24.24 at% are bonded to silicon in the carbidic phase, while 10.01 at% were produced by Equation (1) and remained at the surface. Finally, 11.48 at% of the carbon atoms originate from environment contamination. The whole surface of the particles under scrutinity is determined by summing up the Si-C area from de Si_{2p} spectrum to the O-Si area from the O_{1s} spectrum and to the area from the C-C of C_{1s} spectrum. **Table 5** shows the surface distribution of silicon and carbon bonds and their atomic fractions at SiC surface.

Table 5. Distribution in percentage of surface bonds and atomic fraction at SiC surface.

	Area (%)	Atomic Fraction (%)
Si-C	50.44	24.24
Si-O	24.01	10.01
TOTAL Si (%)		**34.25**
C-C	25.55	21.49
Total area	100	—
Total C (%)		**45.73**

3.4. Zeta Potential Measurement

The change in zeta-potential values as a function of pH for Si and SiC particles is shown in **Figure 8**.

Changes in zeta potential are set in the light of the functional groups present on silicon and silicon carbide surfaces. In the pH range investigated, the acid and basic forms of the water are H_3O^+ and H_2O respectively. To attain comprehension of the zeta potential values, one will highlight all kinds of interactions that could take place between the heterogeneous phases constituted by the solution and the solid particles.

Considering the electronegativity of two atoms of one bond, the less electronegative one presents a negative charge deficiency, $\delta+$, arising from polarization. These sites become the adsorption zones for negative species present in the environment (in the present case, in the solution). They can also attract water molecules, in particular, the free electrons doublet of oxygen. On Si and SiC particles, carbon or silicon atoms bonded with oxygen, more specifically the C-O and Si-O bonds, should exhibit such sites.

Moreover, the electronic structure of graphitic carbon presents two empty 2*p* quanta boxes. These can bind to the doublets of free electrons of the oxygen atom of the hydronium ion, H_3O^+, therefore generating a positive carbon environment.

When the pH of the solution increases, the proportion of the basic form of water rises. Under these conditions, the atoms or functional groups which exhibit LUX-FLOOD acidity [18] will be attacked by the base species of water, namely H_2O. Therefore, the Si $\delta+$ sites interact with H_2O to form silanol groups, as shown in Equation (2).

$$\mathrm{Si-O-Si+H_2O \rightleftharpoons 2Si-OH} \tag{2}$$

In the same way, carbon $\delta+$ sites lead to alcohol groups, Equation (3).

$$\mathrm{C-O-C+H_2O \rightleftharpoons 2C-OH} \tag{3}$$

These reactions induce a change of symmetry of the $\delta+$ polarized site, which passes from two to three.

The symmetry two is formed by the transversal section according to O-Si-O bonds (**Figure 9(a)**). Actives species can approach the silicon site $\delta+$ on both sides.

The symmetry three is oriented by the C3 like axe that represent the Si-OH bonds according to the symmetry of molecules group theory (**Figure 9(b)**). The bond of silicon atom with OH is turned toward the solution while others bonds concern the surface of the particle. In the same order, the number of approach sites for adsorbed negative species also passes from two to three.

Regarding the silicon particles as such and considering the composition of silicon particles surface listed in **Table 2**, the sites exhibiting a $\delta+$ polarization are silicon and carbon atoms when they are bound to oxygen which exhibits a $\delta-$ partial charge. Those sites can adsorb chloride ions or water molecules while hydronium ions can adsorb only on carbon. However, the proportion of carbon that can adsorb hydronium ions is small; it corresponds to 3.03% of the area, which is only 1.38 carbon at% (**Table 3**). So the contribution from theses adsorption processes, bringing positive charges at the surface of the particle are completely surpassed by chloride ions adsorption on silicon $\delta+$ polarized sites.

When the pH increases, the molecules of water tend to react according to Equations (2) and (3), instead of adsorbing on the $\delta+$ polarized sites. As a result, chloride ions are adsorbed to a greater extent and this adsorption process is also enhanced by the silanol and carbon hydroxide formation. Therefore, the zeta potential is expected

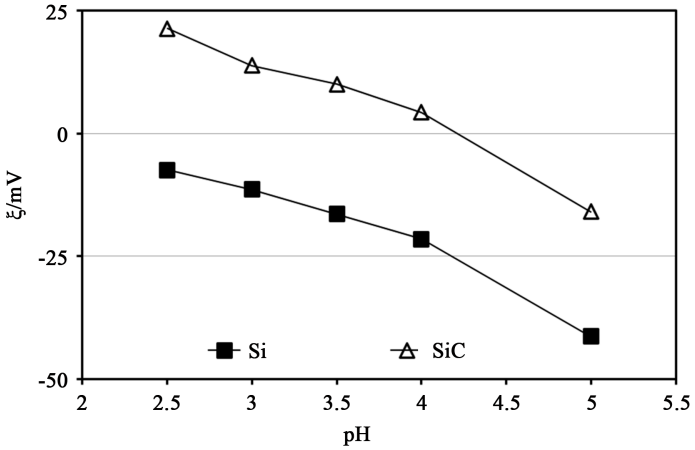

Figure 8. Zeta potential variation vs. pH of the solution for Si and SiC particles.

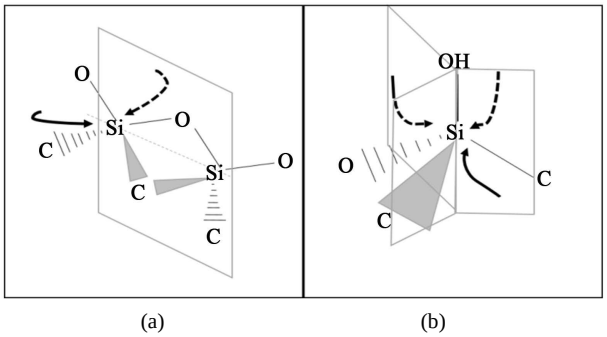

Figure 9. Si-O and Si-OH plans permitting passing from symmetry two (a) to three (b).

to become more and more negative with pH increasing as observed in the experimental results presented in **Figure 8**.

Silicon carbide presents Si-O bonds involving only 11.05 at% of silicon. These latter ones are $\delta+$ charged due to polarization. Additionally, free carbon atoms C, representing 22.35 at%, can adsorb hydronium ions so that, the total charge remains positive at the surface of the particles. As the pH increases, the proportion of hydronium ions in solution decreases as well as its adsorption rate on carbon. The total surface charge becomes less and less positive. Concurrently, the reaction of silanol formation (Equation (2)) occurs due to the pH increase. In fact hydroxyl ions concentration increases with the pH.

The adsorption of chloride ions also contribute to rise the negative surface charge, so that the total positive surface charge of the particles decreases. This trend continues until the potential of zero charge (PZC) is reached at pH 4.2. The PZC obtained in this work is close to that reported by Xiao *et al.* [19] for SiC particles dispersed in KCl 0.01 M. At this pH, the SiC particles surface displaythe same amount of positive charge than negative charges, leading therefore to a neutral particles surface charge.

For pH values higher than 4.2, the hydronium ions activity is drastically reduced and therefore their adsorption. The adsorption of negative charges at the surface is ensured by chloride ions. This adsorption increases due to the three order symmetry that the silicon offers. The zeta potential becomes more and more negative.

4. Conclusions

A thorough characterization of Si and SiC particles was conducted in the present study in order to understand the surface chemistry of these materials. The study of the infrared spectra of the particles enabled the identification of functional groups at the particles surfaces. These were confirmed by the XPS measurements. Indeed, the compositions in atomic and mass percentage of the particles surfaces have been resolved on the basis of a global

XPS spectra, while, the high resolution spectra obtained by peaks deconvolution allowed the identification of the various bonds in which atoms are involved. Peak areas integration by the method of isosceles triangle has been found to be suitable to assess the atomic percentages as well as the proportions of the various bonds were established. Thus silicon particles are respectively covered by 54.85% and 36.85% of Si-O and Si-Si bonds. The rest being zeolite remaining from the raw material used. Silicon carbide SiC surface is constituted for 50.44% of Si-C bonds, for 24.01% of Si-O bonds. Graphite represents 25.55% of the surface.

The determined surface functional groups and the physicochemical interactions that they are susceptible to be responsible for are consistent with the zeta potential variation with respect to the pH of the solution. In fact, zeta potential measures suggest, for both materials, the adsorption of hydronium and chlorine ions and water molecules present in solution. Adsorption of chlorine ions and water molecules give to silicon particle negatives zeta potential values. In the case of silicon carbide, adsorption of hydronium ions results to positive zeta potential until a pH of 4.2. Finally, the surface state in terms of atomic percentages, is consistent with the variation of zeta potential.

Acknowledgements

All authors are very thankful for the kind help and fruitful discussion provided by P. Bowen (EPFL, LTP) and C. Morais (EPFL, LTP). D.M.K Abro is very thankful to the Swiss Government for the economic support provided through the “Swiss Government Excellence Scholarship” (No. 2012.067/Côte d’Ivoire/OP), which made possible the present work.

References

[1] Fellner, P. and Cong, P.K. (1996) Ni-B and Ni-Si Composite Electrolytic Coatings. *Surface Coatings Technology*, **82**, 317-319. http://dx.doi.org/10.1016/0257-8972(96)02738-7

[2] Yeh, S.H. and. Wan, C.C. (1994) Codeposition of SiC Powders with Nickel in a Watts Bath. *Journal of Applied Electrochemistry*, **24**, 993-1000. http://dx.doi.org/10.1007/BF00241190

[3] Kılıç, F., Gül, H., Aslan, S., Alp, A. and Akbulut, H. (2013) Effect of CTAB Concentration in the Electrolyte on the Tribological Properties of Nanoparticle SiC Reinforced Ni Metal Matrix Composite (MMC) Coatings Produced by Electrodeposition. *Colloids Surfaces A*: *Physicochemical and Engineering Aspects*, **419**, 53-60. http://dx.doi.org/10.1016/j.colsurfa.2012.11.048

[4] Benea, L., Luigi, P., Borello, A. and Martelli, S. (2002) Wear Corrosion Properties of Nano-Structured SiC-Nickel Composite Coatings Obtained by Electroplating. *Wear*, **249**, 995-1003. http://dx.doi.org/10.1016/S0043-1648(01)00844-4

[5] Hou, K.H., Ger, M.-D., Wang, L.M. and Ke, S.T. (2002) The Wear Behaviour of Electro-Codeposited Ni-SiC Composites. *Wear*, **253**, 994-1003. http://dx.doi.org/10.1016/S0043-1648(02)00222-3

[6] Rudnik, E., Burzyńska, L., Dolasiński, Ł. and Misiak, M. (2010) Electrodeposition of Nickel/SiC Composites in the Presence of Cetyltrimethylammonium Bromide. *Applied Surface Science*, **256**, 7414-7420. http://dx.doi.org/10.1016/j.apsusc.2010.05.082

[7] Socha, R.P., Laajalehto, K. and Nowak, P. (2002) Influence of the Surface Properties of Silicon Carbide on the Process of SiC Particles Codeposition with Nickel. *Colloids Surfaces A*: *Physicochemical and Engineering Aspects*, **208**, 267-275. http://dx.doi.org/10.1016/S0927-7757(02)00153-X

[8] Brunauer, S., Emmett, P. and Teller, E. (1938) Adsorption of Gases in Multimolecular Layers. *Journal of the American Chemical Society*, **60**, 309-319. http://dx.doi.org/10.1021/ja01269a023

[9] Bocanegra, E.P., Chauveau, C. and Gökalp, I. (2007) Experimental Studies on the Burning of Coated and Uncoated Micro and Nano-Sized Aluminium Particles. *Aerospace Science and Technology*, **11**, 33-38. http://dx.doi.org/10.1016/j.ast.2006.10.005

[10] De Seres, L.-P. (2007) Adsorption des contaminants de l’eau blanche sur des silices colloïdales. Ph.D. Thesis, Université du Québec.

[11] Higashi, G.S., Chabal, Y.J., Trucks, G.W. and Raghavachari, K. (1990) Ideal Hydrogen Termination of the Si (111) Surface. *Applied Physics Letters*, **56**, 656. http://dx.doi.org/10.1063/1.102728

[12] Rumyantsev, V.V. (1971) Identification of Characteristic Energy Losses upon Scattering of Fast Electrons at Large-Angles. *Physical Letters A*, **36**, 213-214. http://dx.doi.org/10.1016/0375-9601(71)90427-0

[13] Moreau, O. (2006) Synthèse de greffons organiques à fonctionnalités antimicrobiennes. Greffage sur wafer de silicium. Aspects physico-chimiques de l’adhesion particulaire. Ph.D. Thesis, Bologna Université de Reims-Champagne Ar-

denne.

[14] Binner, J. (2001) Characterization of Silicon Carbide and Silicon Powders by XPS and Zeta Potential Measurement. *Journal of Materials Science Letters*, **20**, 123-126. http://dx.doi.org/10.1023/A:1006734100499

[15] Meier, W.M., Olson, D.H. and Baerlocher, C. (1996) Atlas of Zeolite Structural Types. Elsevier.

[16] Gupta, A., Paramanik, D., Varma, S. and Jacob, C. (2004) CVD Growth and Characterization of 3C-SiC Thin Films. *Bulletin of Material Science*, **27**, 445. http://dx.doi.org/10.1007/BF02708562

[17] Ramis, G., Quintard, P. and Cauchetier, M. (1989) Surface Chemistry and Structure of Ultrafine Silicon Carbide: An FT-IR Study. *Journal of American Ceramic Society*, **72**, 1962-1967. http://dx.doi.org/10.1111/j.1151-2916.1989.tb06304.x

[18] Flood, H. and Förland, T. (1947) The Acidic and Basic Properties of Oxides. *Acta Chimica scandinavica*, **1**, 592-604. http://dx.doi.org/10.3891/acta.chem.scand.01-0592

[19] Xiao, C., Ni, Q., Chen, H. and Guo, L. (2012) Effect of Polyvinylpyrrolidone on Rheology of Aqueous SiC Suspensions Dispersed with Poly(aspartic acid). *Colloids and Surfaces A*: *Physicochemical and Engineering Aspects*, **399**, 110. http://dx.doi.org/10.1016/j.colsurfa.2012.02.046